Current Biology 20, 1093–1098, June 22, 2010 ©2010 Elsevier Ltd All rights reserved DOI 10.1016/j.cub.2010.04.041

Report

DAP1, a Novel Substrate of mTOR, Negatively Regulates Autophagy

Itay Koren,[1] Eran Reem,[1] and Adi Kimchi[1,*]
[1]Department of Molecular Genetics, Weizmann Institute of Science, Rehovot 76100, Israel

Summary

Autophagy, a catabolic process responsible for the degradation of cytosolic components, is upregulated when nutrient supplies are limited [1]. A critical step in autophagy induction comprises the inactivation of a key negative regulator of the process, the Ser/Thr kinase mammalian target of rapamycin (mTOR) [2]. Thus far, only a few substrates of mTOR that control autophagy have been identified, including ULK1 and Atg13 [3–5], both of which function as positive mediators. Here we identify death-associated protein 1 (DAP1) as a novel substrate of mTOR that negatively regulates autophagy. The link of DAP1 to autophagy was first apparent in that its knockdown enhanced autophagic flux and in that it displayed a rapid decline in its phosphorylation in response to amino acid starvation. Mapping of the phosphorylation sites and analysis of phosphorylation mutants indicated that DAP1 is functionally silenced in growing cells through mTOR-dependent phosphorylations on Ser3 and Ser51. Inactivation of mTOR during starvation caused a rapid reduction in these phosphorylation sites and converted the protein into an active suppressor of autophagy. These results are consistent with a "Gas and Brake" model in which mTOR inhibition also controls a buffering mechanism that counterbalances the autophagic flux and prevents its overactivation under nutrient deprivation.

Results and Discussion

DAP1 Is a Highly Conserved Proline-Rich Phosphoprotein

Human *DAP1* gene encodes a single abundant mRNA transcript (2.4 kb in size), which is ubiquitously expressed in many types of cells and tissues [6]. The predicted open reading frame of *DAP1* corresponds to a small protein of 102 amino acids in length, rich in prolines (15%), and lacking any identifiable motifs (Figure 1A). A single 17 kDa protein is translated in cells from the corresponding Flag-tagged cDNA, and endogenous DAP1 protein runs as a single 15 kDa protein (see Figure S1A available online). In vivo labeling of HeLa cells with ^{33}[P]-orthophosphate, followed by immunoprecipitation from cells, revealed that DAP1 is a phosphoprotein in growing cells (Figure S1B). Through database search, it was found that DAP1 is highly conserved in evolution, and orthologs were identified in most eukaryotes (Figures S1C and S1D).

Amino Acid Starvation Increases the Electrophoretic Mobility of DAP1 on Gels, Indicative of Its Reduced Phosphorylation

Several stress conditions were applied to HeLa cells to identify a cellular setting in which DAP1 may be regulated. We found that, following amino acid starvation, an increase in the steady-state levels of the protein was observed, accompanied by an enhanced electrophoretic mobility on gels (Figure 1B). These two regulatory events characterizing the DAP1 protein response to amino acid deprivation were detected in all cell lines tested, including human (HeLa, MCF7, HEK293), monkey (COS-7), and mouse (B16, SV40 immortalized MEFs, 35-8) cell lines (Figure 1C).

The increase in DAP1 protein levels occurred as early as 2–4 hr after culturing HeLa cells in media lacking amino acids (EBSS), and it persisted for at least 24 hr (Figure 1B; Figure S2A). The strong increase in protein levels was associated with only a small elevation in mRNA levels (Figure 1B), suggesting that additional posttranscriptional regulatory processes may take place as well. DAP1 is a stable protein with a turnover that exceeds 10 hr (Figure S2B), thus ruling out the possibility that the rapid increase in protein steady-state levels results from protein stabilization. Notably, the increase in DAP1 protein takes place under conditions in which overall protein translation is suppressed [7, 8]. As seen in Figure S2C, the short-lived p14ARF protein declined at the same time DAP1 protein was upregulated. Moreover, the increase in DAP1 protein levels during amino acid deprivation was prevented by cycloheximide (data not shown). Thus, in contrast to the majority of cellular proteins, DAP1 protein translation continues and is even upregulated in response to amino acid starvation.

The second level of DAP1 regulation, comprising the focus of this work, involves the apparent changes in its electrophoretic mobility on gels. The fast-migrating form of DAP1, which appeared concomitant with the disappearance of the slow-migrating form characteristic of nutrient-rich conditions, occurred as early as 0.5–2 hr after shifting the cultures to EBSS and persisted for the entire starvation period (Figure S2A). The dynamics of the changes in DAP1 electrophoretic mobility are very rapid. Refeeding of the starved cells with amino acids resulted in a fast upshift of the DAP1 band as early as 0.5–1 hr post refeeding (Figure 1D; see also Figure 2E). The identification of DAP1 as a phosphoprotein by in vivo phosphorylabeling (Figure S1B) suggests that the change in electrophoretic mobility may represent a change in the phosphorylation state of the protein. To test this, we immunoprecipitated DAP1 from cells that were either starved of amino acids or grown in nutrient-rich conditions, and we treated the captured protein with the generic calf intestinal alkaline phosphatase (CIP). Treatment of DAP1 immunoprecipitated from control unstarved cells with CIP resulted in the appearance of the fast-migrating form, whereas the slow-migrating form disappeared. Notably, this new band appeared at the same position as DAP1 immunoprecipitated from starved cells, with or without CIP treatment (Figure 1E), suggesting that the faster form observed upon starvation is in fact dephosphorylated DAP1. Thus, DAP1 is phosphorylated in nutrient-rich conditions and undergoes dephosphorylation upon amino acid starvation.

Mapping DAP1 Phosphorylation Sites

In order to map one or more DAP1 phosphorylation sites, we generated stable cell lines of HEK293 cells that express

*Correspondence: adi.kimchi@weizmann.ac.il

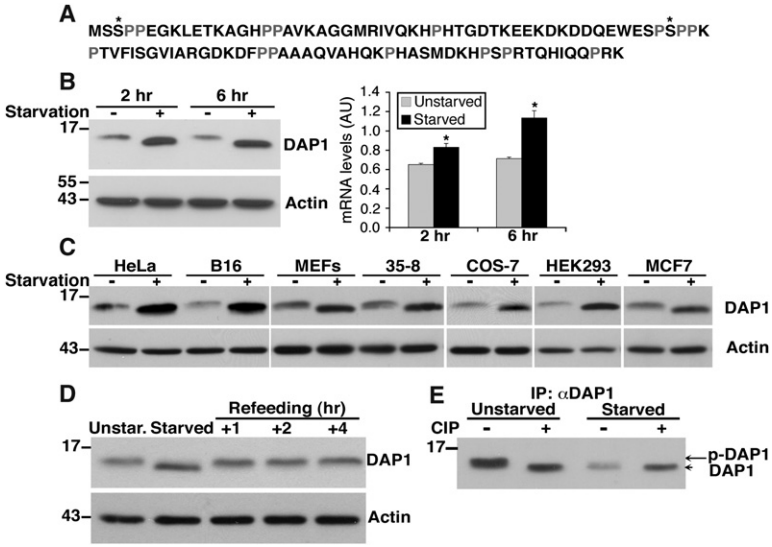

Figure 1. DAP1 Is Regulated at the Expression and Phosphorylation Levels during Nutrient Starvation

(A) Human DAP1 amino acid sequence. Proline residues are marked in gray. Serines 3 and 51 are marked with asterisks.

(B) DAP1 protein levels and the corresponding mRNA steady-state levels were measured by western blot analysis and real-time polymerase chain reaction, respectively, following amino acid starvation for 2 or 6 hr. Data presented are the mean ± standard deviation (SD) calculated from triplicates points. *$p < 0.002$, Student's t test.

(C) DAP1 protein expression following starvation in different cell lines.

(D) DAP1 protein expression in cells that were starved for 4 hr and then supplemented with rich medium for up to 4 hr (refeeding). Actin was used as a loading control in (A)–(D).

(E) Immunoprecipitated DAP1 was incubated in the presence or absence of calf intestinal alkaline phosphatase (CIP) prior to western blot analysis with anti-DAP1 antibody. Arrowhead points to the faster migrating band; arrow points to the slower migrating band.

DAP1 tagged with Flag at the C terminus (DAP1-Flag). Ectopically expressed DAP1-Flag retained its ability to undergo the electrophoretic mobility shift (Figure 2A). Immunopurified DAP1-Flag was either treated or not with CIP, and after resolution on SDS-PAGE, the DAP1-Flag bands were excised and subjected to phosphopeptide mapping analysis by liquid chromatography-tandem mass spectrometry. Ser3 and Ser51 of DAP1 were identified as phosphorylated residues (Figure 1A). In addition, the N-terminal methionine was cleaved, and Ser2 was modified by N-acetylation.

To identify the DAP1 residues that undergo dephosphorylation during starvation, we compared the ratio of phosphorylated and nonphosphorylated peptides in DAP1 immunoprecipitated from extracts of unstarved cells versus starved cells. This comparison revealed that Ser51 is dephosphorylated during starvation (Figure 2B). Notably, technical difficulties prevented the detection of peptides within the N-terminal third of DAP1 in the starved sample, and therefore the status of the phosphosite on Ser3 during starvation could not be evaluated by this approach.

We next used mutagenesis as a second independent strategy to map the phosphorylated residues that are modified by amino acid starvation. To this end, we tested whether the substitution of Ser3 or Ser51 to Ala or to Asp might abolish the starvation-induced migration shift on gels. In fact, substitution of Ser3 to Ala or Asp (3S/A or 3S/D, respectively) abrogated the gel migration shift responses to starvation (Figure 2C, top). Furthermore, the nonphosphorylatable mutant (3S/A) and the phosphomimetic mutant (3S/D) appeared at the same positions as the dephosphorylated and phosphorylated forms of the wild-type (WT) construct, respectively. These results indicate that Ser3 is also dephosphorylated upon starvation and that the loss of the phosphate residue on this site is responsible for the migration shift on gels. (Because these experiments were performed in transiently transfected cells, variations in steady-state levels of the ectopically expressed proteins are not relevant and vary among experiments).

Notably, the substitution of Ser51 to Ala or Asp (51S/A or 51S/D, respectively) did not abolish the gel migration shift upon starvation (Figure 2C, middle). Thus, the starvation-induced dephosphorylation of Ser51 detected by the mass spectrometry analysis does not confer any conformational or electrostatic changes that can be detected by altered electrophoretic mobility. The double mutants 3,51SS/AA and 3,51SS/DD, as expected, ran on gels in the same pattern as the single mutations of Ser3 (Figure 2C, bottom).

To further follow the fate of Ser51 phosphorylation in cells, we generated anti-phospho-Ser51 antibodies. These antibodies recognize the ectopically expressed WT protein but fail to detect the 51S/A mutant (Figure 2D). At the endogenous level, amino acid starvation resulted in a significant decrease in the phospho-Ser51 signal, whereas total DAP1 protein was markedly elevated at this time point (Figure 2E), indicating by a second independent approach that endogenous DAP1 protein undergoes dephosphorylation on Ser51 during starvation.

Identifying mTOR as the Specific Kinase of DAP1

Reculturing the starved cells in complete medium (refeeding) restored the phosphorylation on both sites, as detected by the return of the slowly migrating band and by the increase in phospho-Ser51 signal (Figure 2E), demonstrating that the changes in Ser3 and Ser51 phosphorylation are very dynamic. These rapid changes in DAP1 phosphorylation state during starvation and refeeding experiments prompted us to search for the specific kinase of DAP1. Notably, DAP1 phosphorylation state on Ser3 and Ser51 correlated with the activity of mTOR in cells, showing a dynamic profile that is similar to other mTOR substrates, such as p70S6K (Figure 2E) and 4E-BP1 (data not shown). Interestingly, Ser3 and Ser51 phosphorylation sites fall within "proline-directed" motifs like those identified in 4E-BP1 [9], which are known to be phosphorylated by mTOR [10, 11]. As a first approach to determine whether DAP1 is phosphorylated by mTOR in vivo, HeLa cells were treated with Torin1, a specific ATP-competitive inhibitor of mTOR [12], and the status of phospho-Ser3 and Ser51 was monitored by the mobility shift of DAP1 in gel and by the decline of the phospho-Ser51 signal, respectively. It was found that the phosphorylation of both Ser3 and Ser51 was strongly attenuated in response to Torin1 treatment (Figure 2F), demonstrating that phosphorylation of DAP1 was significantly attenuated in response to mTOR inhibition in vivo.

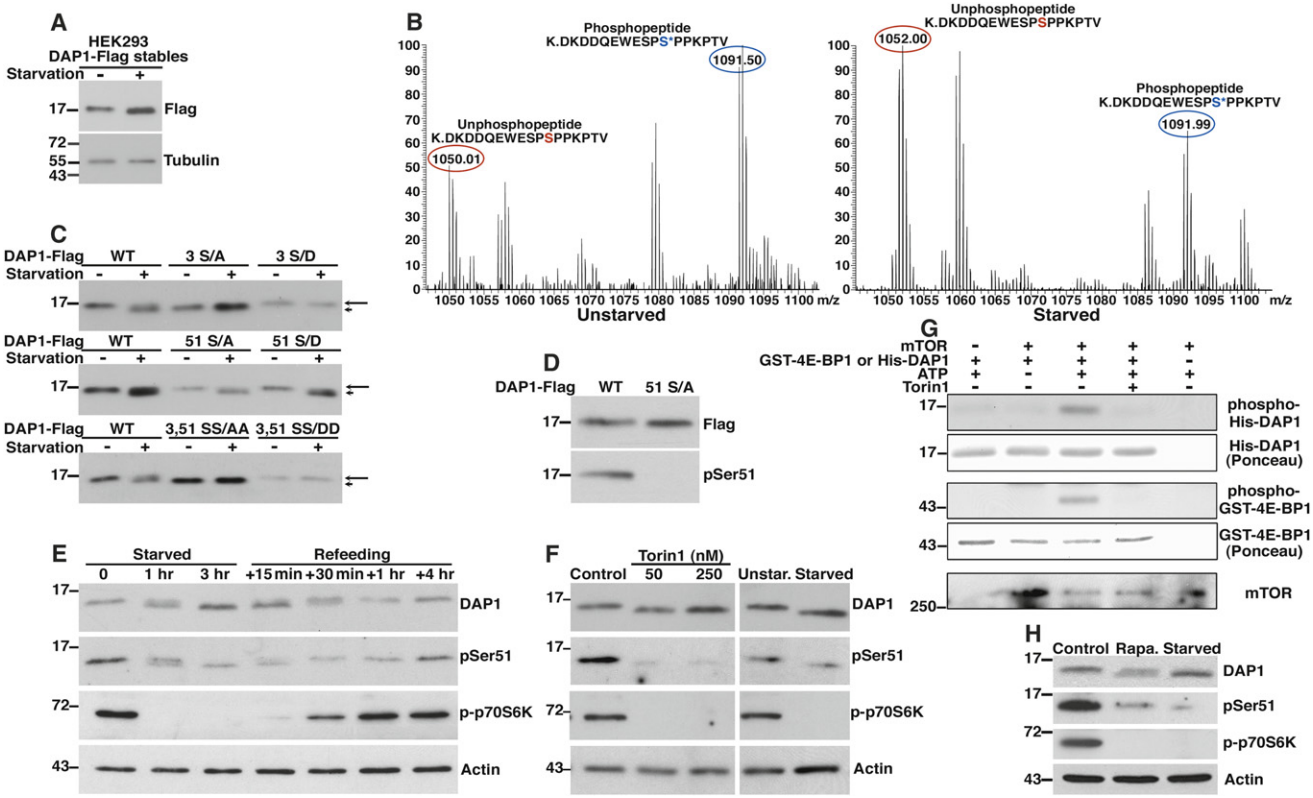

Figure 2. DAP1 Is a Direct Substrate of mTOR

(A) HEK293 polyclonal cells stably expressing DAP1-Flag were cultured in rich medium or were starved for 4 hr, and cell lysates were subjected to western blotting with anti-Flag antibodies. Tubulin was used as a loading control.

(B) The HEK293 polyclonal stable transfectants were either starved or cultured in rich medium for 4 hr, and DAP1-Flag was immunoprecipitated and resolved by SDS-PAGE. The gel was stained with GelCode, and the DAP1-Flag bands in each fraction were excised and analyzed by liquid chromatography-tandem mass spectrometry, as shown in the graphs. Each peak represents a peptide; open red circles mark the unphosphorylated peptides containing Ser51 (marked in red), and open blue circles mark the phosphopeptides containing phosphorylated Ser51 (marked in blue with an asterisk). The graph height represents the relevant abundance of the peptide in the fraction. Left graph, unstarved cells; right graph, starved cells.

(C) HEK293T cells transfected with wild-type (WT) or mutant DAP1 at the indicated residue or residues were cultured in rich medium or starved for 6 hr. Lysates were subjected to western blotting with anti-Flag antibodies. Arrowhead points to the faster migrating band; arrow points to the slower migrating band.

(D) HeLa cells transfected with WT or Ser51Ala mutant DAP1-Flag were cultured in rich medium or starved for 6 hr. Lysates were subjected to western blotting with anti-Flag and anti-phospho-Ser51 DAP1 (pSer51) antibodies.

(E) Lysates from HeLa cells that were starved for 3 hr and then recultured in complete medium (refeeding) for up to 4 hr were subjected to western blotting with anti-DAP1, anti-phospho-Ser51 DAP1 (pSer51), and anti-phospho-Thr389 p70S6K (p-p70S6K) antibodies.

(F) HeLa cells were treated with Torin1 or dimethyl sulfoxide (control) or were cultured in rich medium (unstarv.) or in EBSS (starved) for 3 hr. Lysates were subjected to western blotting as in (E).

(G) Immunopurified mTOR (bottom) was incubated with recombinant His-DAP1 or GST-4E-BP1 in the presence or absence of ATP or Torin1. Equal quantities of substrates assayed were verified by Ponceau staining.

(H) HeLa cells were treated with EBSS (starved) or with 100 nM of rapamycin (rapa.) for 2 hr, and cell lysates were subjected to western blotting as in (E).

Phosphoryaltion of p70S6K, used as a positive control, was similarly affected by Torin1.

Next, endogenous mTOR was immunoprecipitated from HEK293T cells and subjected to in vitro kinase assays with bacterially produced recombinant His-DAP1 or GST-4E-BP1 as substrates. Figure 2G shows that mTOR phosphorylates His-DAP1 on Ser51, as detected by the anti-phospho-Ser51 antibody. GST-4E-BP1 phosphorylation was monitored by using anti-phospho-Thr37/46 antibody. Additionally, the phosphorylation of both substrates was attenuated in vitro in the presence of Torin1, proving that purified cellular mTOR directly phosphorylates DAP1. Notably, mTOR exists in cells in two multiprotein complexes, mTOR complex 1 (mTORC1) and mTORC2, the former displaying strong sensitivity to the drug rapamycin [2]. Figure 2H shows that treatment with rapamycin resulted in dephosphorylation of both Ser3 and Ser51 of DAP1, demonstrating that mTORC1 phosphorylates DAP1 in cells.

DAP1 Knockdown Increases Autophagy

To study the functional outcome of DAP1 knockdown on autophagy induced by nutrient deprivation, we generated polyclonal and monoclonal HeLa cells stably expressing GFP-LC3. *LC3*, one of the autophagy (Atg) genes involved in autophagosome formation, associates with the autophagosome membrane in its lipidated form, thus serving as a marker for autophagosomes [13, 14].

DAP1 was knocked down in the GFP-LC3 polyclonal stable clones before exposing the cells to EBSS. As shown in Figures 3A and 3B, during starvation there is a strong increase in the

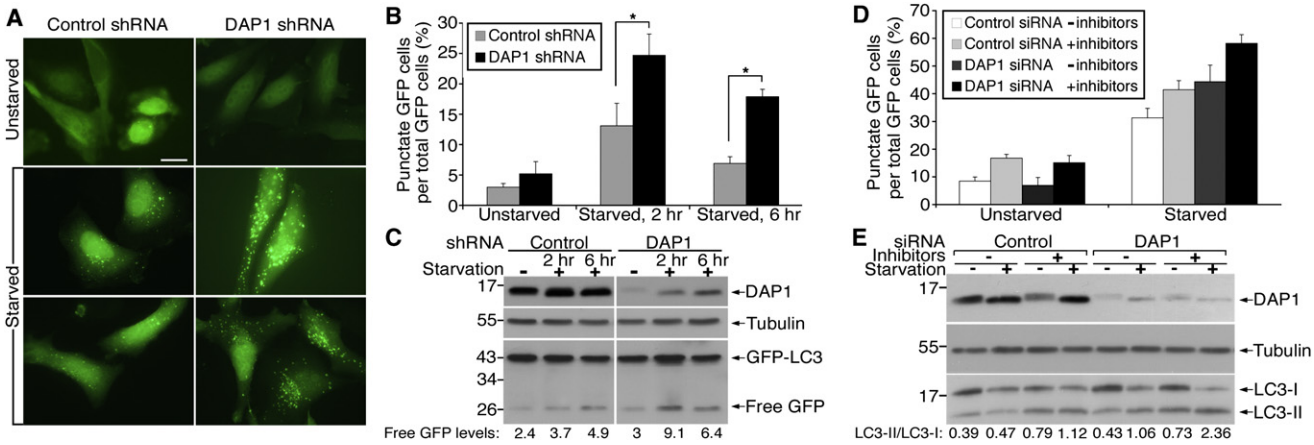

Figure 3. DAP1 Knockdown Increases Autophagic Flux

(A) A polyclonal population of HeLa cells stably expressing GFP-LC3 was transfected with DAP1-targeting small hairpin RNA (shRNA) or HcRed shRNA as control for 5 days and then starved for 2 or 6 hr. Cells were fixed with 3.7% formaldehyde and were analyzed by fluorescent microscopy. Scale bar represents 20 μm.

(B) Quantitation of the percentage of cells with punctate GFP-LC3 fluorescence per total GFP-LC3-positive cells. Data represent mean ± SD calculated from triplicates of 100 transfected cells each. *$p < 0.02$.

(C) Western blot analysis with indicated antibodies of extracts from GFP-LC3 stably expressing cells transfected with DAP1 or HcRed shRNA. The quantified values of free GFP levels for each sample are indicated at the bottom.

(D) HeLa cells stably expressing GFP-LC3 (clone 7) were transfected with DAP1 or HcRed small interfering RNA (siRNA) for 3 days and then either cultured in rich medium or starved in the presence or absence of lysosomal inhibitors (E64d [10 μg/ml] + pepstatin A [10 μg/ml]) for 4 hr. Cells were fixed as in (A) and analyzed as in (B).

(E) Western blot analysis of cell extracts prepared from siRNA-transfected cells (clone 7) reacted with the indicated antibodies. The ratio of LC3-II/LC3-I measured for each sample is indicated at the bottom.

number of cells displaying punctate fluorescent staining per total GFP-LC3-positive cells in DAP1 knockdown cells in comparison to control small hairpin RNA (shRNA) cells. Western blot analysis demonstrated that as early as 2 hr after starvation, free GFP accumulated to a greater extent in cells lacking DAP1 (Figure 3C). During starvation, autophagosomal intraluminal GFP-LC3 is degraded in the autolysosomes, and free GFP accumulates because it is relatively stable to lysosomal proteases. Thus, increased accumulation of free GFP in DAP1 knockdown cells reinforces the point that knockdown of DAP1 increases autophagic activity rather than blocking later stages of autolysosome maturation or degradation. Similar acceleration of autophagosome formation was obtained when the knockdown experiments were performed in a GFP-LC3 monoclonal stable cell line (clone 7) and with another DAP1 shRNA vector to exclude off-target effects (Figures S3A–S3C). Autophagy was also quantified by automated software measuring the total area of GFP-LC3 puncta per cell. Figure S3D demonstrates that, during starvation, the total area of GFP-LC3 puncta per cell is significantly increased by the knockdown of DAP1 in comparison to control small interfering RNA (siRNA) cells.

These results were also confirmed by western blotting for endogenous LC3, which, when conjugated to phosphatidylethanolamine (LC3-II), migrates as a faster form on gels (at 16 kDa versus 18 kDa for the unconjugated LC3-I). DAP1 knockdown by either one of the two shRNAs caused a significant increase in the LC3-II/LC3-I ratio, as detected at 2 and 4 hr of amino acid deprivation (Figure S3E), indicating that DAP1 knockdown accelerated autophagosome formation. Inhibitors of lysosomal activity (E64d and pepstatin A) did not abrogate the stimulatory effect of DAP1 knockdown on autophagy, but rather contributed to a significant, further elevation in the GFP-LC3 punctate staining ($p < 0.03$, t test, DAP1 siRNA + inhibitors versus DAP1 siRNA − inhibitors) (Figure 3D). In addition, the ratio between LC3-II and LC3-I on blots was elevated in DAP1-depleted cells during starvation and increased even more when the lysosomal inhibitors were added (Figure 3E). These results prove that the increased accumulation of autophagosomes in cells lacking DAP1 results from enhancement of autophagic activity rather than from blockage of late stages of the process.

In conclusion, the knockdown experiments performed using three different DAP1 RNA interference constructs (two shRNAs and one siRNA pool), several clones of GFP-LC3 stably expressing cells, and a few methods to monitor autophagy suggest that DAP1 plays a suppressive role in the autophagy process.

Dephosphorylation of DAP1 Activates the Suppressive Function of the Protein in Autophagy

In order to test whether the dephosphorylation of DAP1 activates or inactivates the autophagic suppressive effects, the WT DAP1, phosphomimetic (3,51SS/DD), or nonphosphorylatable (3,51SS/AA) mutants were introduced into GFP-LC3 transfectants in which the endogenous protein was knocked down by using an individual siRNA that targets the 3′ untranslated region (UTR) of DAP1 mRNA. These siRNAs, although effective against the endogenous DAP1, did not affect the ectopically expressed mutants that were generated from a DAP1 construct that lacks the 3′UTR (Figure 4B). During starvation, the 3,51SS/AA mutant blocked the increase in autophagosome accumulation observed upon knockdown of DAP1, whereas the 3,51SS/DD mutant failed to restore the response to the level of the control siRNA transfected cells (Figure 4A). Notably, the overexpressed WT protein was also active in these experiments, because it underwent strong dephosphorylation. These results demonstrate that the dephosphorylated form of DAP1 is the active form that suppresses autophagy.

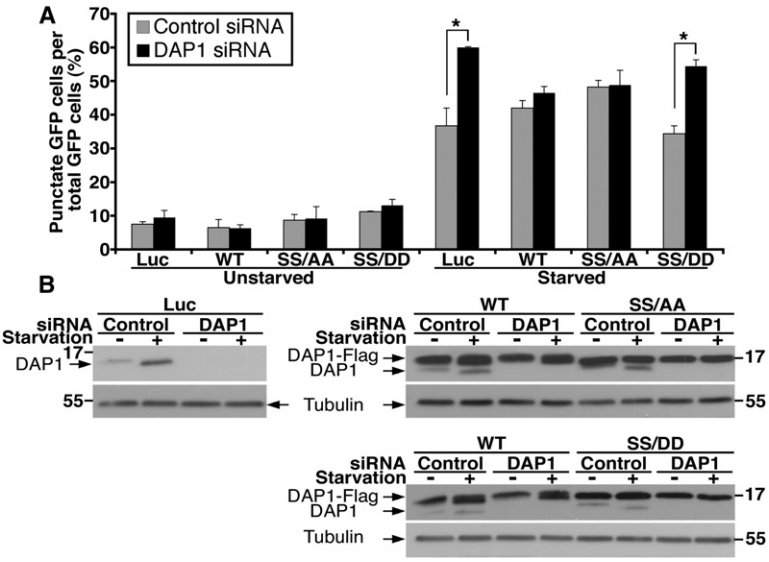

Figure 4. Dephosphorylation of DAP1 Activates Its Suppressive Function in Autophagy

(A) Clone 7 GFP-LC3 HeLa cells were cotransfected with siRNA to endogenous DAP1 or HcRed, together with luciferase (Luc), WT, or mutated DAP1-Flag plasmids, for 3 days and were then either cultured in rich medium (unstarved) or starved of amino acids for 4 hr. Cells were fixed and analyzed by fluorescence microscopy. Graph indicates the percentage of cells with punctate GFP-LC3 fluorescence per total GFP-LC3-positive cells as a mean ± SD calculated from triplicates of 100 transfected cells each. *$p < 0.03$. (Note that statistical comparison of the various control siRNA-expressing cells under starvation, including those expressing the nonphosphorylatable mutant [3,51SS/AA] [gray bars, right, starved], indicated no significant difference in autophagosome accumulation).

(B) Western blot analysis of lysates from (A) reacted with anti-DAP1 or anti-Tubulin (as loading control) antibodies.

In light of data showing that other mTOR substrates such as DEPTOR or PRAS40, which are regulated by mTOR, also in turn control mTOR activity [15–17], it was of interest to test whether a bidirectional interaction might also exist in the case of DAP1. In this model, the functional dephosphorylated form of DAP1 would negatively regulate autophagy by enhancing mTOR activity, and therefore its knockdown should further suppress mTOR activity during autophagy. To this end, we knocked down DAP1 in GFP-LC3 stably expressing cells that were either starved or treated with rapamycin, and we used the phosphorylation status of 4E-BP1 and p70S6K to evaluate mTOR activity in cells. Figure S4A shows the expected increase in autophagic activity in DAP1 knockdown cells during both starvation and rapamycin. However, mTOR activity was not affected by DAP1 knockdown, and the reduction in 4E-BP1 phosphorylation, as monitored by the nonphospho-Thr46 antibody and by the migration shifts identified by total 4E-BP1 antibody, was not further enhanced by knocking down DAP1 (note that p70S6K is completely dephosphorylated upon induction of autophagy and therefore was not a useful marker in these experiments) (Figure S4B). Based on these results, we conclude that DAP1, a substrate of mTOR, does not feed back on mTOR activity upon its dephosphorylation.

Altogether, this work highlights the important role that DAP1 has in autophagy regulation. Some preliminary in vivo documentation of the involvement of DAP1 in autophagy was recently provided in a planarian remodeling system in which expression of the planarian *DAP1* ortholog is activated in the population of cells undergoing autophagy during the remodeling/regeneration process [18]. To date, little is known about suppressors of autophagy, and only a few have been identified, including mTOR and several members of the Bcl-2 family [2, 19, 20]. In this work, we have identified DAP1 as a suppressor of autophagy and as a novel substrate of mTOR. We propose that its suppressive function, acquired once the inhibitory phosphorylations are removed by mTOR inactivation, may restrict the intensity of the autophagic flux to maintain the continuous benefits of this process under stress. Notably, another way to balance the extent of autophagy is by turning off p70S6K, a positive mediator of autophagy, through mTOR inhibition [21]. The conversion of DAP1 into an active suppressor of autophagy by dephosphorylation fits a "Gas and Brake" model in which mTOR, the main regulator of autophagic induction, also simultaneously controls the activity of a specific balancing brake aimed at limiting the extent of the autophagic response to maintain the proper homeostatic balance.

Supplemental Information

Supplemental Information includes Supplemental Experimental Procedures and four figures and can be found with this article online at doi:10.1016/j.cub.2010.04.041.

Acknowledgments

We thank S. Bialik for her continuous advice and for reading and discussing the manuscript. We thank S. Ben-Dor from the Bioinformatics and Biological Computing Unit at the Weizmann Institute of Science for performing the bioinformatics analysis. We thank G. Jona, Director of the Protein Purification Center at the Weizmann Institute of Science, for expression and purification of recombinant proteins. We thank The Smoler Proteomic Center (Technion, Haifa, Israel) for performing the mass spectrometry analysis. This work was supported by the Kahn Fund for Systems Biology at the Weizmann Institute of Science, by a Center of Excellence grant from the Flight Attendant Medical Research Institute, and by a grant from the European Union FP7 to APO-SYS. A.K. is the incumbent of the Helena Rubinstein Chair of Cancer Research.

Received: January 28, 2010
Revised: April 18, 2010
Accepted: April 19, 2010
Published online: May 27, 2010

References

1. Yang, Z., and Klionsky, D.J. (2010). Mammalian autophagy: Core molecular machinery and signaling regulation. Curr. Opin. Cell Biol. *22*, 124–131.
2. Laplante, M., and Sabatini, D.M. (2009). mTOR signaling at a glance. J. Cell Sci. *122*, 3589–3594.
3. Jung, C.H., Jun, C.B., Ro, S.H., Kim, Y.M., Otto, N.M., Cao, J., Kundu, M., and Kim, D.H. (2009). ULK-Atg13-FIP200 complexes mediate mTOR signaling to the autophagy machinery. Mol. Biol. Cell *20*, 1992–2003.
4. Ganley, I.G., Lam, H., Wang, J., Ding, X., Chen, S., and Jiang, X. (2009). ULK1.ATG13.FIP200 complex mediates mTOR signaling and is essential for autophagy. J. Biol. Chem. *284*, 12297–12305.

5. Hosokawa, N., Hara, T., Kaizuka, T., Kishi, C., Takamura, A., Miura, Y., Iemura, S., Natsume, T., Takehana, K., Yamada, N., et al. (2009). Nutrient-dependent mTORC1 association with the ULK1-Atg13-FIP200 complex required for autophagy. Mol. Biol. Cell *20*, 1981–1991.
6. Deiss, L.P., Feinstein, E., Berissi, H., Cohen, O., and Kimchi, A. (1995). Identification of a novel serine/threonine kinase and a novel 15-kD protein as potential mediators of the gamma interferon-induced cell death. Genes Dev. *9*, 15–30.
7. Dann, S.G., and Thomas, G. (2006). The amino acid sensitive TOR pathway from yeast to mammals. FEBS Lett. *580*, 2821–2829.
8. de Haro, C., Méndez, R., and Santoyo, J. (1996). The eIF-2alpha kinases and the control of protein synthesis. FASEB J. *10*, 1378–1387.
9. Gingras, A.C., Raught, B., Gygi, S.P., Niedzwiecka, A., Miron, M., Burley, S.K., Polakiewicz, R.D., Wyslouch-Cieszynska, A., Aebersold, R., and Sonenberg, N. (2001). Hierarchical phosphorylation of the translation inhibitor 4E-BP1. Genes Dev. *15*, 2852–2864.
10. Burnett, P.E., Barrow, R.K., Cohen, N.A., Snyder, S.H., and Sabatini, D.M. (1998). RAFT1 phosphorylation of the translational regulators p70 S6 kinase and 4E-BP1. Proc. Natl. Acad. Sci. USA *95*, 1432–1437.
11. Gingras, A.C., Gygi, S.P., Raught, B., Polakiewicz, R.D., Abraham, R.T., Hoekstra, M.F., Aebersold, R., and Sonenberg, N. (1999). Regulation of 4E-BP1 phosphorylation: A novel two-step mechanism. Genes Dev. *13*, 1422–1437.
12. Thoreen, C.C., Kang, S.A., Chang, J.W., Liu, Q., Zhang, J., Gao, Y., Reichling, L.J., Sim, T., Sabatini, D.M., and Gray, N.S. (2009). An ATP-competitive mammalian target of rapamycin inhibitor reveals rapamycin-resistant functions of mTORC1. J. Biol. Chem. *284*, 8023–8032.
13. Kabeya, Y., Mizushima, N., Ueno, T., Yamamoto, A., Kirisako, T., Noda, T., Kominami, E., Ohsumi, Y., and Yoshimori, T. (2000). LC3, a mammalian homologue of yeast Apg8p, is localized in autophagosome membranes after processing. EMBO J. *19*, 5720–5728.
14. Mizushima, N., Yamamoto, A., Hatano, M., Kobayashi, Y., Kabeya, Y., Suzuki, K., Tokuhisa, T., Ohsumi, Y., and Yoshimori, T. (2001). Dissection of autophagosome formation using Apg5-deficient mouse embryonic stem cells. J. Cell Biol. *152*, 657–668.
15. Peterson, T.R., Laplante, M., Thoreen, C.C., Sancak, Y., Kang, S.A., Kuehl, W.M., Gray, N.S., and Sabatini, D.M. (2009). DEPTOR is an mTOR inhibitor frequently overexpressed in multiple myeloma cells and required for their survival. Cell *137*, 873–886.
16. Oshiro, N., Takahashi, R., Yoshino, K., Tanimura, K., Nakashima, A., Eguchi, S., Miyamoto, T., Hara, K., Takehana, K., Avruch, J., et al. (2007). The proline-rich Akt substrate of 40 kDa (PRAS40) is a physiological substrate of mammalian target of rapamycin complex 1. J. Biol. Chem. *282*, 20329–20339.
17. Sancak, Y., Thoreen, C.C., Peterson, T.R., Lindquist, R.A., Kang, S.A., Spooner, E., Carr, S.A., and Sabatini, D.M. (2007). PRAS40 is an insulin-regulated inhibitor of the mTORC1 protein kinase. Mol. Cell *25*, 903–915.
18. González-Estévez, C., Felix, D.A., Aboobaker, A.A., and Saló, E. (2007). Gtdap-1 promotes autophagy and is required for planarian remodeling during regeneration and starvation. Proc. Natl. Acad. Sci. USA *104*, 13373–13378.
19. Maiuri, M.C., Le Toumelin, G., Criollo, A., Rain, J.C., Gautier, F., Juin, P., Tasdemir, E., Pierron, G., Troulinaki, K., Tavernarakis, N., et al. (2007). Functional and physical interaction between Bcl-X(L) and a BH3-like domain in Beclin-1. EMBO J. *26*, 2527–2539.
20. Pattingre, S., Tassa, A., Qu, X., Garuti, R., Liang, X.H., Mizushima, N., Packer, M., Schneider, M.D., and Levine, B. (2005). Bcl-2 antiapoptotic proteins inhibit Beclin 1-dependent autophagy. Cell *122*, 927–939.
21. Scott, R.C., Schuldiner, O., and Neufeld, T.P. (2004). Role and regulation of starvation-induced autophagy in the Drosophila fat body. Dev. Cell *7*, 167–178.